Neural, Parallel & Scientific Computations 10 (2002) 339-354

A Galerkin Spectral Method for Thermo-Convection Boundary Value Problems

N. C. Papanicolaou and C. I. Christov

Department of Mathematics, University of Louisiana at Lafayette,

Lafayette, LA 70504-1010, USA

Abstract

In the present work we develop a Galerkin spectral technique for solving coupled higher-order boundary value problems arising in continuum mechanics. The set of the so-called beam functions are used as a basis together with the harmonic functions. As a featuring example we treat the convective flow of a viscous liquid in a vertical slot. We show that the rate of convergence of the series is fifth-order algebraic for the different unknown functions. Though algebraic, the fifth order rate of convergence is fully adequate for the generic problems under consideration, which makes the new technique a useful tool in numerical approaches to convective problems. For a limited range of the governing parameters, we derive asymptotic expansions for the sought functions and find these to be in good agreement with our numerical results.

Keywords: spectral methods, beam functions, natural convection, perturbation methods

MSC 2000: 37L65, 74S25, 76M22, 76E06, 76R10

1. INTRODUCTION

Fourth-order boundary value problems are the standard model in continuum mechanics arising both in elasticity and in viscous liquid dynamics. The simplified 1D models are respectively the beam equations and Poiseuille flow. A method developed for one of the fields can easily be applied to the other. The numerical treatment of multi-dimensional problems of mechanics of continua can be much more complicated because of the fact that the models are not evolutionary systems (Cauchy-Kovalevskaya type) and that the boundary-value problems are of higher order. Both these difficulties can be alleviated if a suitable spectral technique is developed in the sense that the basis set of functions satisfies all the boundary conditions.

Received August 07, 2002

Naturally, a basis system of functions which does not satisfy all the boundary conditions, such as the Fourier functions, would exhibit very poor convergence near the boundaries, where the solution must satisfy four boundary conditions. An elucidating discussion on the performance of different sets of functions for various problems can be found in the encyclopedic book of Boyd [2].

In the present work we embark on developing spectral techniques involving the so-called *beam functions* first introduced by Lord Rayleigh, see [12]. Some preliminary account about the new technique can be found in [10, 6].

While the spectral approach to single-equation models is well developed, this is not the case when the main dynamical equation is coupled to an equation for temperature or for some other state variable. In the last case the boundary value problem for the additional sought function can differ from the one for the main unknown function. For the sake of definiteness we will focus our attention on thermal convection in a vertical slot, which is a generalization of the Poiseuille flow.

The Galerkin spectral expansion is verified for internal consistence and shown to have fifth-order algebraic rate of convergence. In order to have an independent verification of the performance of the algorithm we find a perturbation approximate solution of boundary-layer type for both the temperature and stream function. Separate expressions are found for the boundary and outer layer and then these are matched yielding uniform approximate solutions valid for the whole interval $[-1,1]$. These results verify the solutions obtained using our numerical technique.

2. THERMAL CONVECTION IN A VERTICAL SLOT

Consider the 2D flow in a vertical slot with a linear vertical temperature gradient, differentially heated walls, and subject to modulation of gravity in the vertical direction. The problem definition is well-described in the literature (refer to [1, 7, 5, 10] and Fig. 1 for a definition sketch). The notation used is standard:

$$x = \frac{x^*}{L} - 1, \quad y = \frac{y^*}{L}, \quad \omega = \omega^* \frac{L^2}{\kappa}, t = t^* \omega^*, \quad \psi = \frac{\psi^*}{\nu}, \quad \theta = \frac{T^*}{\delta T} + x - \tau_B y,$$

where ν is the kinematic viscosity, κ — the thermal diffusivity, $2L$ — the width of the slot, and δT — the horizontal temperature difference. The asterisk denotes dimensional variables, while the same notation without an asterisk stands for the respective dimensionless quantity.

The Rayleigh number Ra, the Prandtl number Pr, and stratification parameter, γ, are defined as:

$$Ra = \frac{\beta g_0 \delta T L^3}{\nu\kappa}, \quad Pr = \frac{\nu}{\kappa}, \quad 4\gamma^4 = \tau_B Ra,$$

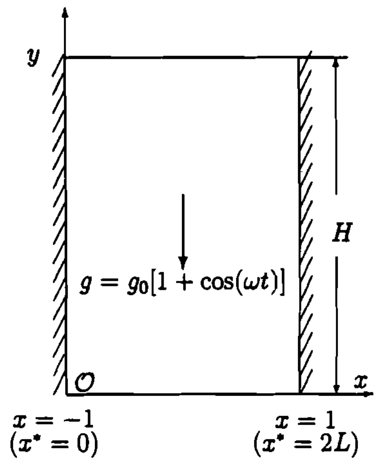

Figure 1: Flow Geometry.

where β is the coefficient of thermal expansion of the liquid, g_0 – the mean gravity, ε – the dimensionless amplitude of gravity modulations, ω – the dimensionless frequency, and τ_B is the dimensionless vertical temperature gradient. Using a finite difference operator splitting scheme, the 2D flow is investigated numerically in [5]. We focus our attention on the 1D case for the purposes of developing the new numerical technique.

Under the selected boundary conditions the problem also admits a plane-parallel solution of the form $\Psi(x,t)$, $\Theta(x,t)$ for which the governing system (see [5]) reduces to the following:

$$\frac{1}{Pr}\frac{\partial^3\Psi}{\partial t\partial x^2} = -Ra\left[-1+\frac{\partial\Theta}{\partial x}\right][1+\varepsilon\cos(\omega t)] + \frac{\partial^4\Psi}{\partial x^4}, \tag{2.1}$$

$$\frac{\partial\Theta}{\partial t} = \tau_B\frac{\partial\Psi}{\partial x} + \frac{\partial^2\Theta}{\partial x^2}, \tag{2.2}$$

with boundary conditions

$$\psi = \frac{\partial\psi}{\partial x} = \theta = 0 \quad \text{for} \quad x = \pm 1, \tag{2.3}$$

The 1D flow was first treated in [7], where different régimes of flow were studied. The parametric bifurcation of the 1D solutions was studied in detail in [5] by means of a fully implicit difference scheme and a related 1D problem in [14].

A way out of these difficulties is to use spectral decomposition with respect to complete orthonormal (CON) systems in x-direction. The performance of a spectral method depends heavily on the type of the basis system of functions. The scope of this paper is to implement these ideas for the one-dimensional in space and time-dependent problem (2.1), (2.2), (2.3).

3. THE SPECTRAL TECHNIQUE

The right CON system for a fourth-order problem was introduced by Lord Rayleigh for the problem of vibration of elastic beams. For the specific boundary conditions arising in viscous liquid dynamics the system and its completeness were discussed in [3]. The product formulas as well as the expansion formulas for the derivatives of different orders were derived in a preceding authors work [4]. The product formula is essential for the application to a nonlinear problem.

3.1. Beam Functions

Consider the Sturm-Liouville problem

$$\frac{d^4u}{dy^4} = \lambda^4 u\,, \quad u = \frac{du}{dy} = 0\,, \quad \text{for} \quad x = \pm 1\,. \tag{3.1}$$

The nontrivial solutions (eigenfunctions) of this problem are given by

$$s_m = \frac{1}{\sqrt{2}}\left[\frac{\sinh\lambda_m x}{\sinh\lambda_m} - \frac{\sin\lambda_m x}{\sin\lambda_m}\right], \qquad \coth\lambda_m - \cot\lambda_m = 0\,, \tag{3.2}$$

$$c_m = \frac{1}{\sqrt{2}}\left[\frac{\cosh\kappa_m x}{\cosh\kappa_m} - \frac{\cos\kappa_m x}{\cos\kappa_m}\right], \qquad \tanh\kappa_m + \tan\kappa_m = 0\,. \tag{3.3}$$

These functions have been introduced by Lord Rayleigh to solve problems arising in elastic-beam theory and they are sometimes called beam functions. A major step in the advancement of the application of the beam functions to fluid-dynamics problems was made by Poots [11]. The magnitudes of the different eigenvalues can be found in most of the above cited works from the literature.

Chandrasekhar [3] derived their counterparts for problems with cylindrical symmetry. For applications to stability problems, see also [8, 13].

The expressions for developing the nonlinear terms into series with respect to the system appeared simultaneously in [9] and [4] though in different form. We stick here to the notations of [4] since they more explicit and easier to verify.

3.2. Expansions for the Derivatives

The different derivatives can be expressed in series with respect to the system as follows:

$$c_n' = \sum_{m=1}^{\infty} a_{nm} s_m\,, \qquad a_{nm} = \frac{4\kappa_n^2\lambda_m^2}{\kappa_n^4 - \lambda_m^4}, \tag{3.4}$$

$$s_n' = \sum_{m=1}^{\infty} \bar{a}_{nm} c_m\,, \qquad \bar{a}_{nm} = \frac{4\kappa_m^2\lambda_n^2}{-\kappa_m^4 + \lambda_n^4}, \tag{3.5}$$

$$c_n'' = \sum_{m=1}^{\infty} \beta_{nm} c_m, \quad \beta_{nm} = \begin{cases} \dfrac{4\kappa_n^2\kappa_m^2}{\kappa_m^4 - \kappa_n^4}\left(\kappa_m \tanh \kappa_m - \kappa_n \tanh \kappa_n\right), & m \neq n, \\ \kappa_n \tan \kappa_n - \left(\kappa_n \tan \kappa_n\right)^2, & m = n, \end{cases} \tag{3.6}$$

$$s_n'' = \sum_{m=1}^{\infty} \bar{\beta}_{nm} s_m, \quad \bar{\beta}_{nm} = \begin{cases} \dfrac{4\lambda_n^2\lambda_m^2}{\lambda_n^4 - \lambda_m^4}\left(\lambda_n \coth \lambda_n - \lambda_m \coth \lambda_m\right), & m \neq n, \\ \lambda_n \coth \lambda_n - \left(\lambda_n \coth \lambda_n\right)^2, & m = n, \end{cases} \tag{3.7}$$

$$c_n''' = \sum_{m=1}^{\infty} d_{nm} s_m, \quad d_{nm} = \frac{4\kappa_n^3\lambda_m^3}{-\kappa_n^4 + \lambda_m^4} \tan \kappa_n \coth \lambda_m, \tag{3.8}$$

$$s_n''' = \sum_{m=1}^{\infty} \bar{d}_{nm} c_m, \quad \bar{d}_{nm} = \frac{4\kappa_m^3\lambda_n^3}{-\kappa_m^4 + \lambda_n^4} \tanh \kappa_m \coth \lambda_n. \tag{3.9}$$

3.3. Products of Beam Functions

For treating nonlinear problems, the most important are the product formulas. Although our featuring example is linear we present these formulas here:

$$c_n(x)c_m(x) = \sum_{k=1}^{\infty} h_k^{nm} c_k(x), \quad \sqrt{2}h_k^{nm} = \sqrt{2}\int_{-1}^{1} c_n(x)c_m(x)c_k(x)\mathrm{d}x \tag{3.10}$$

$$\begin{aligned}
&= \frac{-(\kappa_m + \kappa_k)(\tanh \kappa_m + \tanh \kappa_k) - \kappa_n \tanh \kappa_n}{(\kappa_m + \kappa_k)^2 - \kappa_n^2} \\
&+ \frac{-(\kappa_m - \kappa_k)(\tanh \kappa_m - \tanh \kappa_k) + \kappa_n \tanh \kappa_n}{-(\kappa_m - \kappa_k)^2 + \kappa_n^2} \\
&+ \frac{-(\kappa_m + \kappa_k)(\tanh \kappa_m + \tanh \kappa_k) + \kappa_n \tanh \kappa_n}{(\kappa_m + \kappa_k)^2 + \kappa_n^2} \\
&+ \frac{-(\kappa_m - \kappa_k)(\tanh \kappa_m - \tanh \kappa_k) + \kappa_n \tanh \kappa_n}{(\kappa_m - \kappa_k)^2 + \kappa_n^2} \\
&+ \frac{-(\kappa_n + \kappa_k)(\tanh \kappa_n + \tanh \kappa_k) + \kappa_m \tanh \kappa_m}{(\kappa_n + \kappa_k)^2 + \kappa_m^2} \\
&+ \frac{-(\kappa_n - \kappa_k)(\tanh \kappa_n - \tanh \kappa_k) + \kappa_m \tanh \kappa_m}{(\kappa_n - \kappa_k)^2 + \kappa_m^2} \\
&+ \frac{-(\kappa_n + \kappa_m)(\tanh \kappa_n + \tanh \kappa_m) + \kappa_k \tanh \kappa_k}{(\kappa_n + \kappa_m)^2 + \kappa_k^2} \\
&+ \frac{-(\kappa_n - \kappa_m)(\tanh \kappa_n - \tanh \kappa_m) + \kappa_k \tanh \kappa_k}{(\kappa_n - \kappa_m)^2 + \kappa_k^2},
\end{aligned}$$

$$s_n c_m = \sum_{k=1}^{\infty} f_k^{nm} s_k, \quad s_n s_m = \sum_{k=1}^{\infty} f_m^{nk} c_k, \quad \sqrt{2} f_k^{nm} = \sqrt{2} \int_{-1}^{1} s_n c_m s_k \mathrm{d}x \tag{3.11}$$

$$\begin{aligned}
&= \frac{(\lambda_n + \lambda_k)(\coth\lambda_n + \coth\lambda_k) - \kappa_m \tanh\kappa_m}{(\lambda_k + \lambda_n)^2 - \kappa_m^2} \\
&+ \frac{-(\lambda_k - \lambda_n)(\coth\lambda_k - \coth\lambda_n) + \kappa_m \tanh\kappa_m}{(\lambda_k - \lambda_n)^2 - \kappa_m^2} \\
&+ \frac{-(\lambda_k + \kappa_m)(\coth\lambda_k + \tanh\kappa_m) + \lambda_n \coth\lambda_n}{(\lambda_k + \kappa_m)^2 + \lambda_n^2} \\
&+ \frac{-(\lambda_k - \kappa_m)(\coth\lambda_k - \tanh\kappa_m) + \lambda_n \coth\lambda_n}{(\lambda_k - \kappa_m)^2 + \lambda_n^2} \\
&+ \frac{-(\lambda_n + \kappa_m)(\coth\lambda_n + \tanh\kappa_m) + \lambda_k \coth\lambda_k}{(\lambda_n + \kappa_m)^2 + \lambda_k^2} \\
&+ \frac{-(\lambda_n - \kappa_m)(\coth\lambda_n - \tanh\kappa_m) + \lambda_k \coth\lambda_k}{(\lambda_n - \kappa_m)^2 + \lambda_k^2} \\
&+ \frac{-(\lambda_n + \lambda_k)(\coth\lambda_n + \coth\lambda_k) + \kappa_m \tanh\kappa_m}{(\lambda_k + \lambda_n)^2 + \kappa_m^2} \\
&+ \frac{(\lambda_k - \lambda_n)(\coth\lambda_n - \coth\lambda_k) + \kappa_m \tanh\kappa_m}{(\lambda_k - \lambda_n)^2 + \kappa_m^2}.
\end{aligned}$$

The most obvious test to verify the correctness and consistency of the above derived formulas for the products is to take the product of some two particular functions c_n and c_m and to compare pointwise the products $c_n c_m$ and $s_n c_m$ with their Galerkin expansions into c_k and s_k, respectively. For the products of even functions this comparison is shown in Fig. 2.

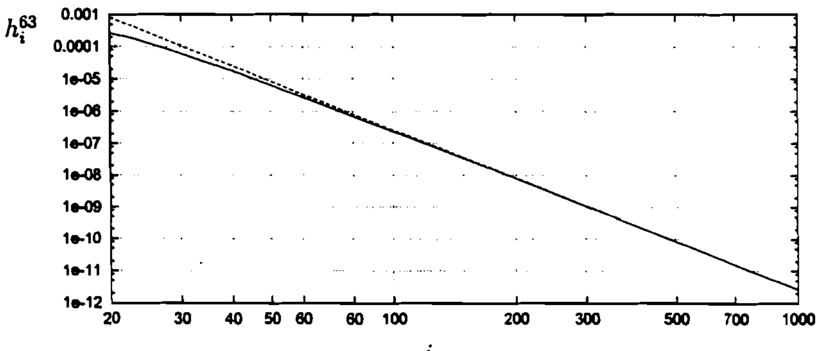

Figure 2: The convergence of the series for the product $c_6 c_3$. Solid line: h_i^{63}; dashed line: the best fit curve $h_i^{63} = 2600\, i^{-5}$.

3.4. Expansion of Unity

We also expanded unity into a c_m series as follows:

$$1 = \sum_{k=1}^{\infty} h_k c_k(x), \quad h_k = \int_{-1}^{1} c_k(x)\mathrm{d}x = \frac{2\sqrt{2}\tanh\kappa_k}{\kappa_k}. \tag{3.12}$$

The convergence of this expansion is algebraic of first order. This is due to the fact that unity does not satisfy the boundary conditions for the beam functions and as a result a strong Gibbs effect is observed near the boundaries.

Yet the overall rate of convergence of the method is fifth-order algebraic, because in the left-hand side of the problems under consideration the fourth power of the respective eigenvalue appears as a multiplier.

3.5. Cross-Expansions between Beam- and Trigonometric Functions

For the convective problem under consideration the difficulties arise from the fact that the boundary value problem for temperature function is of second order, which means that the system of beam functions is not suitable for expanding the temperature field. It is clear that the best suited system for the temperature are the trigonometric *sines* and *cosines*. Hence we need to develop expressions for expanding the beam functions into trigonometric functions and vice versa (see [10, 6]):

$$\sin l\pi x = \sum_{k=1}^{\infty} \sigma_{lk} s_k(x), \quad \sigma_{lk} = \frac{2\sqrt{2}l\pi(\lambda_k)^2(-1)^l}{l^4\pi^4 - \lambda_k^4}, \tag{3.13}$$

$$\cos l\pi x = \sum_{k=1}^{\infty} \chi_{lk} c_k(x), \quad \chi_{lk} = \frac{2\sqrt{2}\kappa_k^3(-1)^{l+1}\tanh\kappa_k}{l^4\pi^4 - \kappa_k^4}, \tag{3.14}$$

$$c_n(x) = \sum_{l=1}^{\infty} \hat{\chi}_{nl} \cos l\pi x, \quad \hat{\chi}_{nl} = \frac{2\sqrt{2}\kappa_n^3(-1)^{l+1}\tanh\kappa_n}{l^4\pi^4 - \kappa_n^4}, \tag{3.15}$$

$$s_n(x) = \sum_{l=1}^{\infty} \hat{\sigma}_{nl} \sin l\pi x, \quad \hat{\sigma}_{nl} = \frac{2\sqrt{2}l\pi(\lambda_n)^2(-1)^l}{l^4\pi^4 - \lambda_n^4}. \tag{3.16}$$

We point out that the convergence when expanding $\cos(l\pi x)$ into c_k series is first order k^{-1} (see (3.14)) due to the fact that it does not satisfy both b.c. for the beam functions. It satisfies the condition on the derivatives but fails to satisfy the conditions on the function itself. Clearly, the situation with the $\sin(l\pi x)$ is better and the rate of convergence is of second order k^{-2} (see (3.13)), because the *sine* functions satisfy the boundary conditions for the functions themselves and the disagreement is more subtle, since the conditions on the first derivative are not satisfied. The situation with the expansions of s_k and c_k in Fourier series is reversed. The order of convergence for c_k is l^{-4} (see (3.15)), and for s_k is l^{-3} (see (3.16)). As it will be shown in what follows, this property is of crucial importance for the overall rate of convergence.

4. THE GALERKIN METHOD

The spectral technique was tested for accuracy and rate of convergence in [10, 6]. Three model ODE problems were solved: A linear fourth order BVP, a nonlinear fourth order BVP and a higher order coupled ODE system. It was found that with only 30 terms in the spectral series the error was of order $O(10^{-8})$ and with 100 terms the error was restricted to a very good order of $O(10^{-10})$. In this section we outline the algorithm for the unsteady thermoconvective flow (the *jitter* flow). For the sake of convenience we introduce the following notations:

$$b_{kl} = \sum_{m=1}^{N} \hat{\sigma}_{ml} a_{km} \tag{4.1}$$

where a_{km} and $\hat{\sigma}_{ml}$ are from (3.4) and (3.16), respectively.

For the time approximation we use a staggered in time Crank-Nicolson-type scheme

$$\sum_{j=1}^{N} \beta_{ij} \frac{p_i^{n+1} - p_i^n}{\tau Pr} = -Ra \left[\sum_{l=1}^{N} \pi l \chi_{li} d_l^{n+\frac{1}{2}} - \frac{2\sqrt{2}\tanh \kappa_i}{\kappa_i} \right] [1 + \varepsilon \cos(n\omega\tau)] + \kappa_i^4 \frac{p_i^{n+1} + p_i^n}{2} \tag{4.2}$$

$$\frac{d_l^{n+\frac{3}{2}} - d_l^{n+\frac{1}{2}}}{\tau} = \tau_B \sum_{j=1}^{N} b_{jl} p_j^{n+1} - l^2\pi^2 \frac{d_l^{n+\frac{3}{2}} - d_l^{n+\frac{1}{2}}}{2} \tag{4.3}$$

where $\{p_i\}_{i=1}^N$, $\{d_l\}_{l=1}^N$ are the spectral coefficients of the stream function and temperature respectively and the superscripts denote the time stage.

Following the method demonstrated by Boyd in [2], we can show that the convergence rate of our solutions is fifth order algebraic. First, we show the following lemma relative to the BVP (2.1)-(2.3) :

Lemma 1 $\Theta(x,\cdot) \in C^5\,([-1,1])$.

Proof: Since $\Psi \in C^4([-1,1])$, then $\Psi_x \in C^3([-1,1])$. As a result we get from (2.2) that $\Theta_{xx} \in C^3([-1,1])$ which gives $\Theta \in C^5([-1,1])$.

Theorem 1 *Suppose* $\Psi(x,\cdot)$, $\Theta(x,\cdot) \in C^5\,(\,[-1,1]\,)$. *Then, the convergence rate of both the spectral series for the solution of problem (2.1), (2.2), (2.3) is fifth order algebraic.*

Proof: The spectral series for the stream function and temperature are given by

$$\Psi(x,t) = \sum_{k=1}^{K} p_k c_k(x), \quad \Theta(x,t) = \sum_{k=1}^{K} d_k \sin(k\pi x) \tag{4.4}$$

respectively. We prove the theorem for Ψ since the proof for Θ can be carried out in like fashion. By definition,

$$p_k = \int_{-1}^{1} c_k(x)\Psi(x,\cdot)\,\mathrm{d}x \tag{4.5}$$

After successive integrations by parts, acknowledging the boundary conditions and the characteristic equation $\tanh\kappa_k + \tan\kappa_k = 0$, and making use of (2.3) we get

$$p_k = \left[\frac{\Psi_{xxxx}}{\sqrt{2}\kappa_k^5}\left(\frac{\sinh\kappa_k x}{\cosh\kappa_k} - \frac{\sin\kappa_k x}{\cos\kappa_k}\right)\right]_{x=-1}^{x=1} - \frac{1}{\sqrt{2}\kappa_k^5}\int_{-1}^{1}\left(\frac{\sinh\kappa_k x}{\cosh\kappa_k} - \frac{\sin\kappa_k x}{\cos\kappa_k}\right)\Psi_{xxxxx}\,\mathrm{d}x. \tag{4.6}$$

Due to the lack of differentiability of Ψ beyond the fifth order the last term will contribute in the integration by part quantities which are not trivially equal to zero. Hence, continuing the process will not cancel the terms of order κ_m^5.

Note that in the proof for Θ the main reason for stopping after the fifth integration by parts is that the term that corresponds to the first term in (4.6) is non-zero.

Q.E.D.

5. THE LIMITING CASE: $\omega \sim O(1)$, $\varepsilon \leq 1$

Apart from proving its internal consistence, rate of approximation, and convergence, the best verirification of a numerical method is to compare its prediction to an analytical solution in some limiting cases. As has been noted previously, the problem (2.1), (2.2), (2.3) does not posses an exact analytic solution. However, for $\omega \sim O(1)$, $\varepsilon \leq 1$ it can be treated by perturbation technique and approximate analytic solutions can be found for these values of our parameters. It has been pointed out in [5] that the magnitude of the parameter of vertical stratification γ ($4\gamma^4 = \tau_\beta Ra$) plays a most important role in defining the profiles of the velocity and temperature. For the sake of convenience we incorporate the large parameter Ra in the scalings and rewrite our coupled system of equations in terms of $\psi = \Psi/Ra$

$$\frac{1}{Pr}\frac{\partial^3\psi}{\partial t\partial x^2} = -\left[-1 + \frac{\partial\theta}{\partial x}\right][1 + \varepsilon\cos(\omega t)] + \frac{\partial^4\psi}{\partial x^4}, \tag{5.1}$$

$$\frac{\partial\theta}{\partial t} = 4\gamma^4\frac{\partial\psi}{\partial x} + \frac{\partial^2\theta}{\partial x^2}, \tag{5.2}$$

with boundary conditions:

$$\psi(-1) = \psi(1) = 0, \quad \psi_x(-1) = \psi_x(1) = 0 \quad \text{and} \quad \theta(-1) = \theta(1) = 0 \tag{5.3}$$

We separate the spatial interval into two areas. The "inner" layer (or boundary layer near the vertical walls) and the "outer" layer in the core of the flow. We denote $\delta = 1/\gamma$ which will be the small parameter of our perturbation solution.

5.1. The Outer Layer

So, the solutions of (5.1) and (5.2), Ψ and Θ outside the boundary layer are given by the perturbation expansions:

$$\Psi = \Psi_0 + \delta\Psi_1 + \delta^2\Psi_2 + \dots, \tag{5.4}$$

$$\Theta = \Theta_0 + \delta\Theta_1 + \delta^2\Theta_2 + \dots. \tag{5.5}$$

Substituting (5.4) and (5.5) into (5.1) and equating like terms we obtain:

$$\frac{1}{Pr}\Psi_{0,txx} = (1 - \Theta_{0_x})(1 + \varepsilon\cos\omega t) + \Psi_{0,xxxxx}. \tag{5.6}$$

Since the spatial derivatives of Ψ are small we have that $\Theta_{0,x} = 1$ which with the use of the symmetry condition $\Theta_0(0) = 0$ yields

$$\Theta_0 = x. \tag{5.7}$$

There is no need to follow the same procedure for Ψ. The reason is that once we have found the uniform expression for θ we may use (5.2) and the suitable boundary conditions for this purpose.

5.2. The Inner Layer

In the inner layer the function changes rapidly and thus ψ_{xxxx} is significant. So, to resolve the inner layer we use the scaled expansions

$$\psi = \delta^3(\phi_0 + \frac{1}{\delta}\phi_1 + \frac{1}{\delta^2}\phi_2 + \dots), \qquad \theta = \theta_0 + \frac{1}{\delta}\theta_1 + \frac{1}{\delta^2}\theta_2 + \dots,$$

where the scaled variable ξ is given by $\delta\xi = x + 1$.

Substituting the last equality into (5.1), (5.2) gives within $O(\delta)$ the system

$$0 = -\theta_{0,\xi}(1 + \varepsilon\cos(\omega t)) + \phi_{0,\xi\xi\xi\xi} \tag{5.8}$$

$$-4\phi_{0,\xi} = \theta_{0,\xi\xi}. \tag{5.9}$$

Combining (5.8) and (5.9) yields the following ODE in ξ since we may treat t as a parameter

$$\theta_{0,\xi\xi\xi\xi\xi} + 4\theta_{0,\xi}(1 + \varepsilon\cos(\omega t)) = 0. \tag{5.10}$$

Subject to the boundary conditions $\theta = \theta_{\xi\xi} = 0$ at $\xi = 0$ and $\lim_{\xi\to\infty}\theta(\xi) < \infty$ we obtain the solution

$$\theta_0^L = C_L(1 - \exp(-a\xi)\cos(a\xi)) \tag{5.11}$$

where $a = a(t) = (1 + \varepsilon\cos(\omega t))^{1/4}$ and C_L is an arbitrary constant to be determined by matching.

In the same fashion near the wall $x = +1$, we introduce the local variable $\xi_R = (1-x)\delta^{-1}$ and hence we get

$$\theta_0^R = C_R(1 - \exp(-a\xi_R)\cos(a\xi_R)). \tag{5.12}$$

5.3. Matching

We introduce an intermediate asymptotic variable $\eta = \sqrt{\delta}\xi$ and rewrite our inner and outer solutions in terms of the new variable.

$$\theta_0^L = C_L(1 - \exp(-a\frac{\eta}{\sqrt{\delta}})\cos(a\frac{\eta}{\sqrt{\delta}})), \qquad \Theta_0 = \sqrt{\delta}\eta - 1. \tag{5.13}$$

Our objective is to determine C_L such that for fixed η, $\lim_{\delta\to 0}(\theta_0^L - \Theta_0) = 0$. Clearly $C_L = -1$ and thus the common part is $cp = -1$. So, the uniform solution for the left boundary layer and the outer layer is

$$\theta^L = \theta_0^L + \Theta_0 - cp = x + \exp\frac{-a(x+1)}{\delta}\cos\frac{a(x+1)}{\delta} + O(\delta). \tag{5.14}$$

We repeat the same procedure for the right boundary layer (near $x = 1$) by setting $x = 1 - \delta\xi$ and obtain the following uniform solution for the right inner and outer layers

$$\theta^R = \theta_0^R + \Theta_0 - cp = x - \exp\frac{a(x-1)}{\delta}\cos\frac{a(1-x)}{\delta} + O(\delta). \tag{5.15}$$

Combining the two uniformly-valid solutions we obtain the uniformly-valid solution for all $x \in [-1, 1]$, we get

$$\theta^u = x + \exp\frac{-a(x+1)}{\delta}\cos\frac{a(x+1)}{\delta} - \exp\frac{a(x-1)}{\delta}\cos\frac{-a(x-1)}{\delta} + O(\delta). \tag{5.16}$$

Using this expression and (5.2) we obtain the following uniform expression for ψ since the integration constant can be easily determined by the boundary conditions

$$\begin{aligned}\psi^u = \frac{1}{4}a\delta^3\{&\exp\frac{-a(x+1)}{\delta}\cos\frac{a(x+1)}{\delta} + \exp\frac{-a(x+1)}{\delta}\sin\frac{a(x+1)}{\delta} \\ &+ \exp\frac{a(x-1)}{\delta}\cos\frac{a(1-x)}{\delta} + \exp\frac{a(x-1)}{\delta}\sin\frac{a(1-x)}{\delta} - 1\} + O(\delta).\end{aligned} \tag{5.17}$$

To compare the perturbation solutions (5.16), (5.16) with the numerical results we juxtapose the graphs of the numerical and asymptotic solutions (see Fig. 3). One sees that the analytical and numerical results are indistinguishable.

We have chosen the case $\gamma = 12$, $\omega = 3$, $\varepsilon = 1$ which is near the border of the parameter range for which our perturbation method is valid. This is a good choice for our purposes since the numerical method fails for vanishingly small values of the

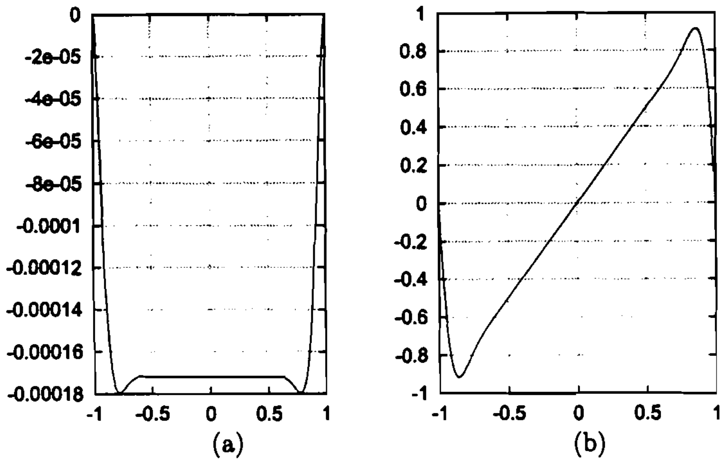

Figure 3: Comparison between spectral (solid lines) and asymptotic (dashed lines) solutions (a) stream function; (b) temperature.

modulation frequency. The reason is that for such small vales of ω a very fine time resolution is required (e.g., 1000 time steps per period) making the algorithm inefficient. Also, for $\varepsilon > 1$ (5.16) and (5.17) become invalid since $a(t) = (1 + \varepsilon\cos(\omega t))^{1/4}$ may become a complex number, thus changing the form of the solution. The snapshots are taken at the end of the period after the stationary oscillations have been reached. The graphs are virtually indistinguishable because the difference is very small, of order $O(10^{-8})$ for Ψ and $O(10^{-5})$ for Θ. We have found this to be the case for all $\omega \leq 3$ and $\varepsilon < 1$.

6. ALGORITHM, RESULTS, AND DISCUSSION

Speaking about the algorithm implementing our scheme we mention that the inversion of the matrix in eq.(4.3) is trivial. The inversion of the matrix in eq.(4.2) is performed just once in the beginning of the algorithm and then the inverse can be used during the time stepping to multiply the r.h.s. of (4.2). This means that the computational cost of the above implicit scheme is equal to the cost of an explicit scheme which makes it highly efficient.

In this section we demonstrate the performance of the method developed. We chose $Pr = 0.73$, $Ra = 5.1165$, $\tau_B = 0.1611$ ($\gamma = 12$) and $\omega = 200$, $\varepsilon = 1$ when stationary oscillations can be reached and we verify numerically that the convergence rate for the unsteady problem is also fifth order algebraic, i.e. $p_k, d_k \sim O(k^{-5})$. In Fig.4 the coefficents p_k and d_k are presented as a function of k.

Let us mention here that the coefficients exhibit the same rate of convergence as

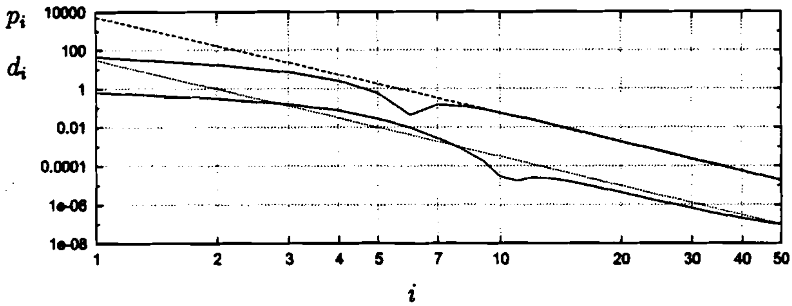

Figure 4: Rate of convergence for $\omega = 200$, $\varepsilon = 1$. Upper solid line: Fourier-Galerkin coefficients of stream function p_i. Accompanying dashed line: the best fit $5350i^{-5}$. Lower solid line: Fourier-Galerkin coefficients of temperature d_i. Accompanying dashed line: the best fit $d_i = 30i^{-5}$.

calculated in the previous section for the sake of comparison with the perturbative solution.

Now we can move to treating the jitter problem as outlined in the precedence. One way to assess the results in this case is to compare with the finite-difference solution from [5]. However, there are some differences between the dimensionless forms of the system as used in [5] and in the present paper. The main one is in the scaling of the spatial variable x. In order to make it more convenient for the spectral derivations we use here the interval $x \in [-1, 1]$ while in [5] the interval is $x \in [0, 1]$. This changes the values of the dimensionless parameters and in the situation of five-dimensional parametric space it becomes unclear to figure out how to scale the values of the dimensionless parameters in order to have the same physical case as the one treated in [5]. The only way we could follow in this situation is to repeat part of the calculations with the finite-difference scheme for the newly defined domain of the independent variable x which is twice larger.

We treat the case with $Pr = 0.73$, $Ra = 51165$, $\tau_B = 0.16112$ ($\gamma = 12$) and $\omega = 200$, $\varepsilon = 1$. The spatial approximation of the scheme has been thoroughly verified in the above and we will not abuse the size of the paper with doing the same for snapshot profiles. What we can do now is to follow the temporal evolution of the solution in one spatial position and to compare with the finite-difference solution. We chose $x = -0.5$ as representative enough position. The most obvious is to take the middle point $x = 0$, but at that point the relative temperature function θ we are using is trivially equal to zero. For the comparisons we take the same number 200 of divisions of one time period in the two numerical algorithms.

Fig. 5 presents the result. The solid lines are the spectral solution, while the dashed ones present the finite-difference solution. In both algorithms we conducted

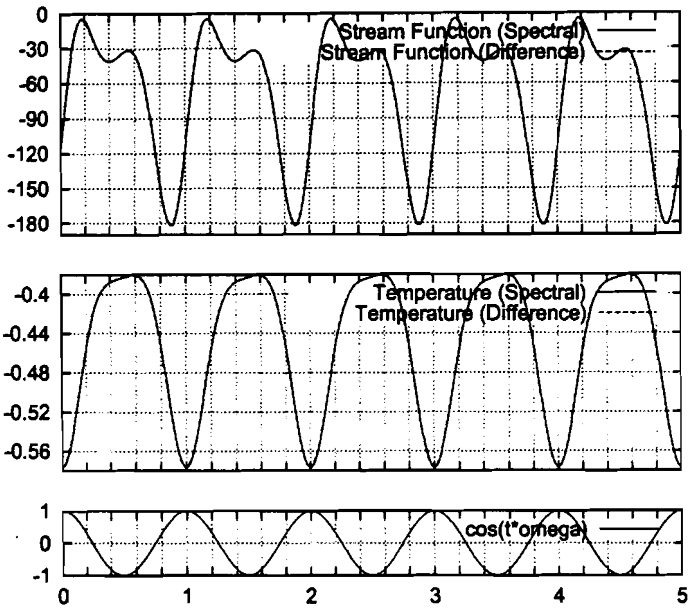

Figure 5: Time-wise comparison between finite-difference and Galerkin solutions for $\omega = 200$ and $\varepsilon = 1$. Uppermost panel: $\Psi(-0.5, t)$; middle panel: $\Theta(-0.5, t)$;lower panel: the loading function $\cos(\omega t)$.

the calculations for 200 time periods in order to ensure that the motion is of type of stationary oscillations and after that we calculated another 5 periods in order to make the comparison between the two solutions. One sees that the agreement is very good quantitatively. The maximum difference is less than 0.1%. We did the same calculations for smaller $\varepsilon = 0.8$ and the result was equally good.

7. CONCLUSIONS

In the present work a Galerkin technique is developed for coupled thermoconvective flows in a vertical slot. The well-known beam functions which satisfy four boundary conditions are used as a basis set for the stream function together with the trigonometric functions for the temperature. The formulas for the cross expansion of the two systems were not available in the literature and are derived here alongside various miscellaneous expressions needed for the successful implementation of the Galerkin technique.

The developed numerical technique is applied to the 1D problem of thermoconvection in a vertical slot with both horizontal and vertical gradients of the temperature. This is a problem with multi-dimensional parametric space which can be attacked only if the algorithm is fast enough like the one proposed here. In order to verify the temporal approximation of the Galerkin scheme we compare the present results to calculations performed using the finite-difference scheme of [5]. The quantitative agreement is very good.

We show theoretically that the convergence rate of the spectral solutions is fifth order algebraic. We verify this by means of a numerical experiment for specific values of the governing parameters. The fifth order means that although algebraic, the convergence is fast enough for all practical purposes. The theoretical and numerical findings are illustrated graphically.

Finally, we treat the case of small modulation frequency both by perturbation technique and numerically. The spectral and analytic results are found to be in good agreement for the common ranges of the governing parameters, for which both techniques are valid. The numerical tool developed can be used for larger frequencies ($O(\gamma^2)$) for which the perturbation method fails.

Thus, a new instrument for numerical investigation of thermoconvective modulated flows is created.

Acknowledgement. The work of N.C.P and C.I.C is supported through Grant No. R199524 by LaSPACE Consortium under LEQSF and NASA Grant NGT5-40035.

REFERENCES

[1] R. F. Bergholz. Instability of steady natural convection in a vertical fluid layer. *J. Fluid Mech.*, 84:743–768, 1978.

[2] J. P. Boyd. *Fourier and Chebyshev Spectral Methods.* Dover, New York, 2000.

[3] S. Chandrasekhar. *Hydrodynamic and Hydromagnetic Instability.* Oxford University Press, Clarendon, London, 1961. Appendix V.

[4] C. I. Christov. A method for treating the stochastic bifurcation of plane Poiseuille flow. *Ann. Univ. Sof., Fac. Math. Mech.*, 76(lb.2 - Mecanique):87–113, 1982/87.

[5] C. I. Christov and G. M. Homsy. Nonlinear dynamics of two dimensional convection in a vertically stratified slot with and without gravity modulation. *J. Fluid Mech.*, 430:335–360, 2001.

[6] C. I. Christov and N. Papanicolaou. Galerkin spectral methods for higher-order boundary-value problems arising in fluid mechanics. In *Proceeding of the Thirtieth Spring Conference of the Union of Bulgarian Mathematicians, Borovets, April 8-11*, pages 438–443, 2001.

[7] A. Farooq and G. M. Homsy. Linear and nonlinear dynamics of a differentially heated slot under gravity modulation. *J. Fluid Mech.*, 313:1–38, 1996.

[8] D. L. Harris and W. H. Reid. On orthogonal functions which satisfy four boundary conditions. I. Tables to use in Fourier-type expansions. *Abstract of Astrophysical Journal, Supplement Series*, III(33):450–450, 1968.

[9] B. S. Jhaveri and F. Rosenberger. Exact triple integrals of beam functions. *J. Comput. Phys.*, 45:300–302, 1982.

[10] N. Papanicolaou and C. I. Christov. Galerkin spectral method for higher-order boundary value problems arising in thermal convection. *Annuaire de l'Universit de Sofia*, 94:71–83, 2000.

[11] G. Poots. Heat transfer by laminar free convection in enclosed plane gas layers. *Quart. J. Mech. Appl. Math.*, 11:357–273, 1958.

[12] Lord Rayleigh. *Theory of Sound*. Dover, New York, 1945.

[13] W. L. Reid and D. L. Harris. On orthogonal functions which satisfy four boundary conditions. II. Integrals to use in Fourier-type expansions. *Abstract of Astrophysical Journal, Supplement Series*, III(33):450–450, 1968.

[14] V. A. Suresh, C. I. Christov, and G. M. Homsy. Resonant thermocapillary and buoyant flows with finite frequency gravity modulation. *Phys. Fluids*, 11:2565–2576, 1999.